

Li and OH-Li Complexes in Hydrothermally Grown Single-Crystalline ZnO

K.M. JOHANSEN,^{1,2} H. HAUG,¹ Ø. PRYTZ,¹ P.T. NEUVONEN,¹
K.E. KNUTSEN,¹ L. VINES,¹ E.V. MONAKHOV,¹ A.YU. KUZNETSOV,¹
and B.G. SVENSSON¹

1.—Department of Physics/Center for Materials Science and Nanotechnology, University of Oslo, P.O. Box 1048, Blindern, 0316 Oslo, Norway. 2.—e-mail: klausmj@fys.uio.no

Fourier-transform infrared spectroscopy (FTIR) and secondary-ion mass spectrometry (SIMS) have been employed to investigate the relation between the Li concentration and the strength of the 3577 cm^{-1} absorption line in five as-grown hydrothermal ZnO wafers. This line has previously been identified as a local vibrational mode of an OH molecule adjacent to a Li atom on the Zn-site. In this work, we show that the integrated absorption of the 3577 cm^{-1} line does not follow the variation in the total Li concentration between different wafers, providing evidence that the concentration is not the limiting factor for the formation of the 3577 cm^{-1} defect. It is speculated that the presence of inhomogeneously distributed Li along the direction of the *c*-axis, as revealed by SIMS depth profiling in three of the studied wafers, is related to trapping of Li by inversion domain boundaries (IDB). IDBs are expected to have high thermal stability, which may be associated with the high apparent thermal stability reported for the 3577 cm^{-1} line.

Key words: ZnO, hydrothermal, lithium, hydrogen, inversion domain boundaries, 3577 , OH-Li complex, secondary-ion mass spectrometry, SIMS, FTIR

Hydrogen and lithium are two important impurities in ZnO, specifically in ZnO grown by the hydrothermal method (HT), where Li is found with concentrations in the range of $1 \times 10^{17}\text{ cm}^{-3}$ to $5 \times 10^{17}\text{ cm}^{-3}$. H acts as a donor, either on interstitial sites or on substitutional O-sites,^{1,2} and may also form complexes with and passivate acceptors.³ Li, on the other hand, act as a donor on the interstitial site and as an acceptor on the substitutional Zn-site, which can be passivated by H. Knowledge about and control of these dopants are, therefore, essential if one seeks to realize stable *p*-type ZnO. In HT-ZnO, the dominating OH-related absorption line⁴ at 3577 cm^{-1} is due to a stretch mode of a OH-bond in the vicinity of Li on a Zn-site (Li_{Zn}).^{3,5} Halliburton et al.³ found from combined FTIR and electron paramagnetic resonance measurements

that 99% of the Li in their samples was contributing to the 3577 cm^{-1} line, i.e., in other words, passivated by H. It is well known that the Li concentration can vary between different as-grown HT-ZnO wafers, and a correlated variation in the integrated absorption coefficient of the 3577 cm^{-1} line may thus be expected. A remarkable feature of the OH-Li complex is the high thermal stability, as it has been reported to be stable at 1200°C during several hours.⁴ This is in strong contrast to that found for other OH-related absorption bands in ZnO, which disappear in the range of 150°C to 750°C .⁶ However, as pointed out by Lavrov et al.,⁷ the temperature stability of the 3577 cm^{-1} band depends on the detailed history of heating and cooling of the sample. This may indicate the involvement of another (in itself highly stable) defect which traps H and Li at low temperatures; when heating the sample H and Li dissociate but are retrapped by the stable defect during cooling down.⁷

In this study, results from Fourier-transform infrared spectroscopy (FTIR) and secondary-ion mass spectrometry (SIMS) have been correlated to investigate the 3577 cm^{-1} absorption line in five different hydrothermally grown ZnO wafers. Both the strength of the 3577 cm^{-1} absorption line and the Li concentration are found to vary from sample to sample, but with no clear correlation between the two. It is also found that the Li concentration is highly nonuniform in three of the samples as a function of depth along the direction of the c -axis, but with no variation along the lateral directions (normal to the c -axis). It is thus considered that the observed inhomogeneity is due to Li decorating defects oriented along the ZnO basal planes normal to the c -axis.

Five hydrothermally grown wafers (labeled A, B, C, D, and E) in their as-grown state, purchased from SPC-Goodwill, were used in this study. The Li concentration ($[\text{Li}]$) was measured by SIMS using a Cameca IMS7f microanalyzer. A primary beam of 10-keV O_2^+ ions was rastered over a surface area of $65\text{ }\mu\text{m} \times 65\text{ }\mu\text{m}$, an electronic gate of 70% of the raster size was used, and the secondary ${}^7\text{Li}^+$ ions were collected from the central part of the sputtered crater ($\sim 30\text{ }\mu\text{m}$ in diameter) for determination of the Li concentration. Crater depths were subsequently measured with a Dektak 8 stylus profilometer, and a constant erosion rate was assumed for depth calibration. The calibration of the Li concentration was performed using an as-implanted sample as reference. The H concentration found in HT-ZnO typically falls below or is close to the SIMS detection limit of $\sim 10^{17}\text{ cm}^{-3}$,⁸ therefore, detailed information about possible variation in the H concentration cannot be obtained. The infrared absorbance spectra were recorded with a Bruker IFS 113v Fourier-transform spectrometer equipped with a global light source, a CaF_2 beamsplitter, and a liquid-nitrogen-cooled InSb detector. The samples were mounted in a closed helium CTI-Gryogenics Helix 22 compressor 8200 cryostat, and the temperature was recorded with a LakeShore Cryotronics DRC 82C temperature controller. Measurements were nominally performed at 20 K, with a spectral resolution of 1 cm^{-1} . Transmission electron microscopy (TEM) studies were performed in a JEOL 2000FX microscope operated at an acceleration voltage of 200 kV. Cross-sectional samples were prepared for the TEM studies using standard grinding and ion-milling techniques.

Figure 1 shows absorption spectra in the as-grown state for all five wafers. The integrated absorption coefficient of the 3577 cm^{-1} line (I_{3577}) is found to be 0.55 cm^{-2} , 1.07 cm^{-2} , 2.21 cm^{-2} , 1.80 cm^{-2} , and 1.83 cm^{-2} for wafers A, B, C, D, and E, respectively. This shows that I_{3577} varies between these wafers by a factor of 4. Unfortunately the detailed history of the wafers is not known, so the variation cannot be directly related to growth procedure, position in the boule, etc.

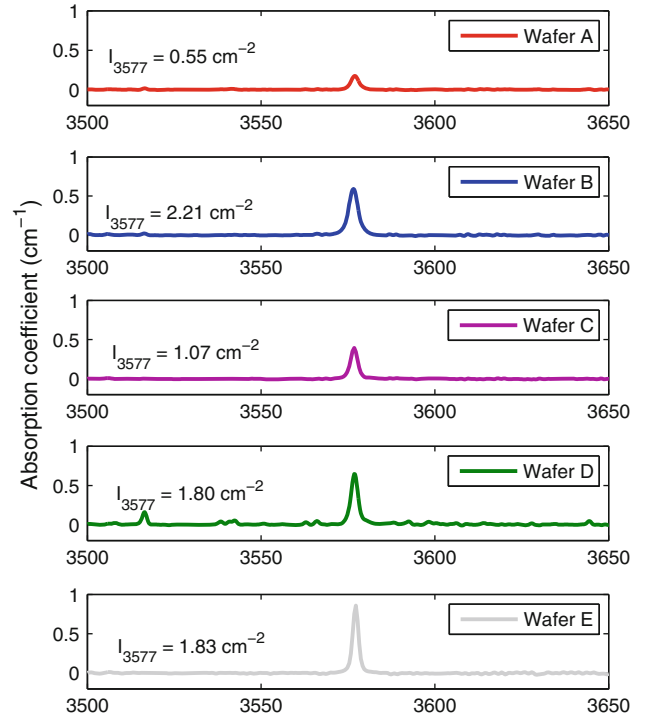


Fig. 1. Infrared absorption spectra measured with light propagating perpendicular to the c -axis ($k \perp \vec{c}$). The integrated absorption coefficient for the 3577 cm^{-1} absorption line is shown to vary from wafer to wafer.

As mentioned, the 3577 cm^{-1} band has previously been identified as a local vibrational OH-stretch mode adjacent to Li_{Zn} , also referred to as the OH-Li complex.³ The variation in absorption strength is directly related to the variation in concentration of the complex:

$$\epsilon_{3577} = \frac{I_{3577}}{c_{3577}}, \quad (1)$$

where ϵ_{3577} is the absorption strength of the OH-Li complex and c_{3577} is the concentration of the same complex. Assuming that only one Li atom takes part in the formation of the OH-Li complex, then $c_{3577} \leq [\text{Li}]$. If 99% of the Li present in the material is involved in the OH-Li complex, as argued by Halliburton et al.,³ one would expect that the variation in I_{3577} should directly reflect $[\text{Li}]$. However, Fig. 2 shows $[\text{Li}]$ as a function of depth in the five different wafers, and the average $[\text{Li}]$ in A, B, C, D, and E is found to be $2.0 \times 10^{17}\text{ cm}^{-3}$, $2.8 \times 10^{17}\text{ cm}^{-3}$, $2.5 \times 10^{17}\text{ cm}^{-3}$, $3.8 \times 10^{17}\text{ cm}^{-3}$, and $2.0 \times 10^{17}\text{ cm}^{-3}$, respectively. In other words, there is no clear correlation between the I_{3577} line and the average $[\text{Li}]$. For instance, wafers A and E, have the same $[\text{Li}]$ while I_{3577} differs by a factor of more than 3. Hence it is concluded that the $[\text{Li}]$ is not the limiting factor in the formation of the OH-Li complex.

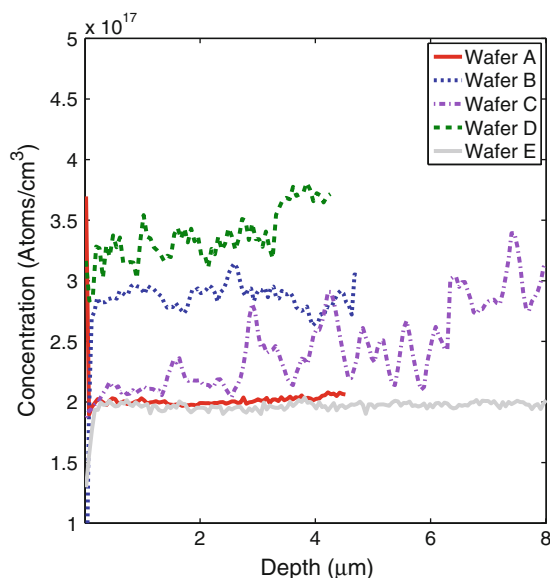


Fig. 2. Li concentration versus depth for five as-grown wafers as measured by SIMS.

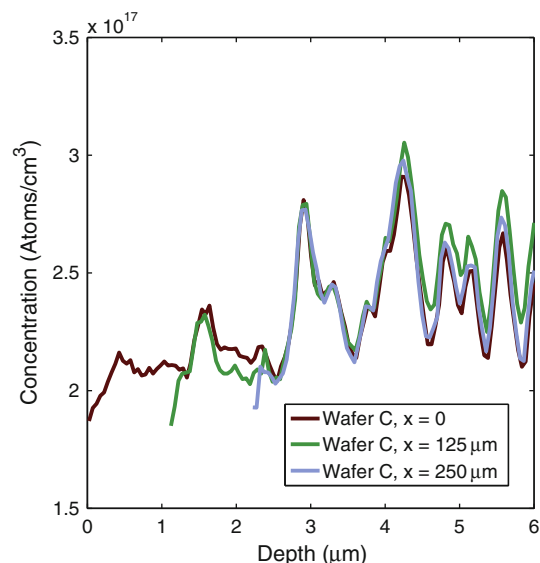


Fig. 3. Li concentration versus depth measured at three different positions (x) of wafer C by SIMS. The depth profiles of the second and third crater is shifted by $1.1 \mu\text{m}$ and $2.2 \mu\text{m}$, respectively, as compared with the first crater due to an offset in the cut angle.

In an attempt to estimate the absorption strength of the OH-Li complex, it is assumed that all of the Li in wafer E contributes to the OH-Li complex. Then a minimum value of $9.3 \times 10^{-18} \text{ cm}$ is obtained for ϵ_{3577} . This value is lower than that reported for another OH-related absorption line in ZnO at 3611 cm^{-1} , $\epsilon_{3611} = 2.46 \times 10^{-17} \text{ cm}$.⁹ This indicates that the true absorption strength might be even higher also for the 3577 cm^{-1} line, with the implication that even in wafer E not all of the Li atoms contribute to the OH-Li complex.

Another interesting feature revealed by Fig. 2 is that in wafers B, C, and D the Li concentration is highly nonuniform as a function of depth along the direction of the c -axis. Interestingly, if different surface positions are investigated on the same wafer, the inhomogeneous features in the Li distribution are almost exactly reproduced except for a shift in depth. An example is shown in Fig. 3, where the Li concentration is depicted as a function of depth for three different crater positions on wafer C. The size of each crater is $65 \mu\text{m} \times 65 \mu\text{m}$ and the three craters are separated by a distance of $125 \mu\text{m}$ from center to center. When the recorded Li distributions for the second and third crater in Fig. 3 are displaced towards larger depths by $1.1 \mu\text{m}$ and $2.2 \mu\text{m}$, respectively, the profiles overlap perfectly. The origin of the shift in depth may be due to a small offset in the angle of the polished surface as compared with the c -axis; estimation of this angle (0.5°) shows that it is close to the specified uncertainty of $\pm 0.25^\circ$ as given by SPC-Goodwill. The angle offset may also explain why these features are normally not observed, since a larger area of secondary-ion acceptance would average out the observed features.

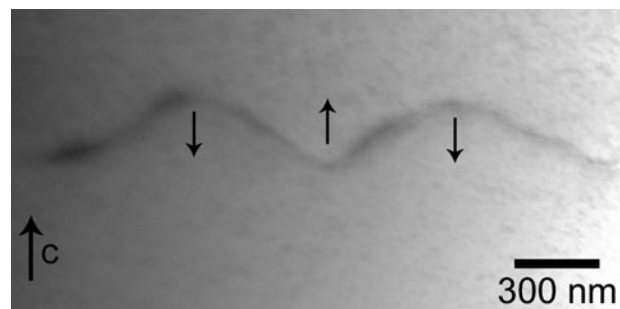


Fig. 4. TEM image of two pyramidal c -axis inversion domains. The orientation of the c -axis is indicated by arrows.

The origin of the observed inhomogeneity in the Li distribution has not yet been established, but a plausible explanation may be that Li decorates defect structures which are confined to the basal planes normal to the c -axis. Interestingly, TEM studies reveal the presence of pyramidal inversion domain boundaries (IDB) (Fig. 4), similar to those observed by Köster-Sherger et al.¹⁰ in Fe-doped ZnO samples. In Ref. 10 it was found that the Fe is primarily present in the IDB. It is thus believed that IDBs may also act as traps for both Li and H, facilitating the formation of the OH-Li complex when the wafer is cooled down after growth or high-temperature processing treatments. In this respect, it is also interesting to note that such inversion domains are expected to have high thermal stability and may, indeed, be part of the explanation of the surprisingly high apparent thermal stability of the

3577 cm^{-1} line and the dependency on the detailed history of heat treatment, as reported by Lavrov et al.⁷

In summary, we have shown that there is no direct correlation between the average Li concentration and the integrated absorption coefficient of the 3577 cm^{-1} line, previously identified as a local vibrational mode originating from a OH-Li complex. Thus the formation of this complex is typically not limited by the concentration of Li. In three of the five investigated wafers the Li distribution is highly inhomogeneous along the direction of the *c*-axis, and the features are reproduced in the lateral directions over the surface. By the use of TEM, one of the wafers with inhomogeneous Li distribution is shown to contain *c*-axis inversion domains, which may be the origin of the inhomogeneous Li distribution acting as strong trapping sites for migrating Li and H atoms. This may also explain the high apparent thermal stability of the 3577 cm^{-1} band by trapping of both Li and H at or in the vicinity of the inversion domain boundaries.

ACKNOWLEDGEMENTS

Support from the FUNMAT@UiO Program and the Norwegian Research Council (FRINAT and NANOMAT Programs) is gratefully acknowledged.

OPEN ACCESS

This article is distributed under the terms of the Creative Commons Attribution Noncommercial License which permits any noncommercial use, distribution, and reproduction in any medium, provided the original author(s) and source are credited.

REFERENCES

1. C.G.V. de Walle, *Phys. Rev. Lett.* 85, 1012 (2000).
2. A. Janotti and C.G.V. de Walle, *Nat. Mater.* 6, 44 (2007).
3. L.E. Halliburton, L. Wang, L. Bai, N.Y. Garces, N.C. Giles, M.J. Callahan, and B. Wang, *J. Appl. Phys.* 96, 7168 (2004).
4. E.V. Lavrov, *Physica B: Condensed Matter* 340–342, 195 (2003).
5. G.A. Shi, M. Stavola, and W.B. Fowler, *Phys. Rev. B Condens. Matter Mater. Phys.* 73, 081201 (2006).
6. E.V. Lavrov, J. Weber, F. Börrnert, C.G.V. de Walle, and R. Helbig *Phys. Rev. B* 66, 165205 (2002).
7. E. Lavrov, F. Börrnert, and J. Weber, *Zinc Oxide A Material for Micro- and Optoelectronic Applications* (Netherlands: Springer, 2005), pp. 133–144.
8. L. Vines, E.V. Monakhov, R. Schifano, W. Mtangi, F.D. Aurret, and B.G. Svensson, *J. Appl. Phys.* 107, 103707 (2010).
9. E. Lavrov, *Physica B: Condensed Matter* 404, 5075 (2009).
10. O. Köster-Scherger, H. Schmid, N. Vanderschaeghe, F. Wolf, and W. Mader, *J. Am. Ceram. Soc.* 90, 3984 (2007).